JOURNAL OF THERMOPHYSICS AND HEAT TRANSFER
Vol. 24, No. 4, October–December 2010

Jet Impingement Heat Transfer from a Circular Cylinder Located Between Confining Walls

Mustahib Imraan* and Rajnish N Sharma†
University of Auckland, Auckland 1142, New Zealand

DOI: 10.2514/1.48171

The heat-transfer characteristics of a circular cylinder (diameter d) located between confining walls (at a varying separation distance of H apart), exposed to a slot jet of air (of width w) from a contoured nozzle, and at a range of spacing z from the jet exit has been studied experimentally and computationally. The study focused on Reynolds numbers Re in the range of 1000–12,000. The results reveal that, while the slot jet impinging on a cylinder in confined space generally yields higher average heat-transfer rates, relative to the uniform crossflow case, these are, however, almost always found to yield lower heat-transfer rates in comparison with corresponding slot-jet impingement without confining walls. It was found that a dimensionless confinement spacing $H/d = 10$ exists that consistently exhibits a minimum in the cylinder heat-transfer rate over all of the nondimensional jet exit to the cylinder spacing z/w and ratio of the cylinder diameter to the slot width d/w that were investigated. It was established that the reduction in heat transfer for confinements H/d between 10 and 16 is due to the jet becoming unstable, thereby periodically flapping across the cylinder, switching between the confining walls, in tandem with vortex shedding from the cylinder. This reduces the effectiveness of impingement and, hence, reduces the heat-transfer rates. It is therefore concluded that jet impingement does not always enhance the heat-transfer rate, but it may, in fact, reduce it under conditions in which the impingement target is located in the midst of confining walls. It was observed that the average of all the Nusselt numbers in a confined space reduces by about 17% when compared with a nonconfined cylinder. In summary, therefore, the influence of confining walls around the cylinder has an unfavorable impact on the flow and, therefore, the heat-transfer rates with jet impingement.

Nomenclature

A_S	=	cylinder surface area, m^2
B	=	constant
d	=	cylinder diameter, m
H	=	spacing between confining walls, m
$\bar{h}$	=	average convective heat-transfer coefficient, $W\,m^{-2}\,K^{-1}$
k	=	thermal conductivity of air, $W\,m^{-1}\,K^{-1}$
m	=	constant
$\overline{Nu}$	=	Nusselt number
Pr	=	Prandtl number
$\dot{Q}_{\text{cond}}$	=	conduction heat-transfer rate through wires, W
$\dot{Q}_{\text{conv}}$	=	convection heat-transfer rate from cylinder surface, W
$\dot{Q}_{\text{diss}}$	=	power dissipation by ohmic heating, W
$\dot{Q}_{\text{rad}}$	=	radiation heat-transfer rate from cylinder surface, W
Re	=	Reynolds number based on cylinder diameter
$\bar{T}_\theta$	=	average cylinder surface temperature, K
T_∞	=	temperature of the air, K
V	=	average jet exit velocity, $m\,s^{-1}$
w	=	slot or slot-jet width, m
z	=	jet-exit-to-cylinder spacing, m
ν	=	kinematic viscosity of air, $m^2\,s^{-1}$

Presented as Paper 2009-4085 at the 41st AIAA Thermophysics Conference, San Antonio, TX, 22–25 June 2009; received 17 November 2009; revision received 12 March 2010; accepted for publication 13 May 2010.

*Ph.D. Candidate, Department of Mechanical Engineering, Private Bag 92019.

†Senior Lecturer, Department of Mechanical Engineering, Private Bag 92019; r.sharma@auckland.ac.nz. Member AIAA.

I. Introduction

JET impingement heat transfer is an aggressive form of heat transfer that involves jets of hot or cold air with high velocity orthogonally striking and impinging on a product or object. The high velocity of the air jet enhances the transport of heat and mass. Consequently, jet impingement yields higher heat-transfer rates than are possible by most other methods of single-phase forced convection. Knowledge of the flow, heat transfer, and forces associated with impinging jets is fundamental to many engineering problems, as it is used in a broad spectrum of industrial applications. Some examples include heat treatment of products, drying of textiles and paper, a variety of manufacturing processes, thermal control of electronics and turbine blades, and in-food engineering to name a few.

There are numerous studies of impingement heat transfer, and application of both numerical and experimental techniques are found in the literature. Jambunathan et al. [1] provided a review of impingement cooling of flat surfaces and highlighted the dependence of heat transfer on jet Reynolds numbers and on the distance from the jet exit to the surface (z). More recently, Narayanan et al. [2] conducted a detailed survey and summarized the experimental literature that exists in relation to fluid mechanics and heat transfer of single-slot jets. The review included past studies on flat, convex, and concave surfaces, as well as those on cylindrical bodies. The reader is directed to [1,2] for further detail.

In the present context of jet impingement heat transfer from a circular cylinder, only a few studies have been reported in the literature. Some early work on impingement heat transfer on a circular cylinder due to an offset and nonoffset slot jet was reported by Sparrow and Alhomoud [3]. It was found that the heat-transfer coefficient increased with slot width and Reynolds number but decreased with slot-to-cylinder separation distance and offset. Flow and heat transfer to a circular cylinder with a hot impinging air jet was investigated by Kang and Greif [4], who also found that heat-transfer rates increased with increasing Reynolds numbers and that the jet width, as well as the slot-to-cylinder separation distance, had a profound effect on heat transfer. The effects of the buoyancy of the jet were also studied, and the idea of an effective Reynolds number was proposed that incorporated a buoyancy contribution. Similar findings

were made by Bartoli et al. [5], who studied jet impingement at a circular cylinder but with a submerged slot jet of water.

Through their experimental work, McDaniel and Webb [6] characterized heat transfer from circular cylinders exposed to slot-jet impingement for Reynolds numbers (based on nozzle average exit velocity and cylinder diameter) in the range 600–8000. Their study also considered cylinder-diameter-to-jet-width ratios d/w of 0.66, 1.0, and 2.0, as well as for the distance from jet-exit-to-cylinder-z-to-nozzle-width w ratio in the range $1 < z/w < 11$. It was found that the slot jet yields higher average heat-transfer rates from the cylinder when compared with uniform crossflow on the basis of identical average velocity in the slot-jet and uniform crossflow configurations. They also found a maximum in heat transfer at $z/w \approx 5$ and explained this to be coincident with the terminal end of the potential core region of the jet, where the strength of the mean flow is still high, and high turbulence levels are also present due to the widening shear layer outside of the thinning potential core. The potential core typically extends to 6–7 jet diameters for circular jets and 4–7 slot widths for rectangular slot jets. Useful empirical correlations for the characteristics of average heat transfer from the cylinder were also offered.

In their investigations of slot-jet impingement cooling of circular cylinders with $d/w = 1$, 2, and 4 in the Reynolds number range of 4000–22,000, Gori and Bossi [7,8] found that the maximum average heat-transfer rate occurs at location $z/w \approx 8$ for a cylinder with $d/w = 4$ and at location $z/w \approx 6$ for a cylinder with $d/w = 2$. The maximum and minimum local heat transfers were found to occur at the front impinging point and 180° at the rear of the cylinder, respectively. The highest average heat-transfer rate was recorded for a cylinder with $d/w = 4$.

Recently, Olsson et al. [9] investigated heat transfer from a slot air jet impinging on a cylinder-shaped food product, placed on a solid surface in a semiconfined area, using computational fluid dynamics (CFD) modeling. This study considered somewhat higher jet Reynolds numbers in the range of 23,000–100,000, with the conclusion that large variations in local Nusselt numbers occur around the cylinder, while the slot-to-cylinder distance z had a low dependency on average heat transfer. The average heat transfer was empirically correlated with the jet Reynolds number, the cylinder-diameter-to-jet-width ratio d/w, and the distance from the jet-exit-to-cylinder-to-nozzle-width ratio z/w. The influence of variations in the partial confinement inherent in their study was not investigated. In a follow-up study, Olsson et al. [10] recently studied flow and heat transfer from multiple slot-jets impinging on circular cylinders and showed the dependence of heat transfer on distance and the opening between jets.

While a good amount of information and knowledge now exists in relation to jet impingement heat transfer, the published literature described and referenced in [1–10] has only considered jets impinging on bodies in free space. The exception being the investigation of Olsson et al. [9], where jet impingement heat transfer was investigated for a circular cylinder placed on a wall. When the range of applications of jet impingement heat transfer is considered, from manufacturing processes through thermal management to food cooling, it becomes patently obvious that impingement processes usually occur on bodies in some form of confined space. In some rapid food-cooling applications, for example, jet impingement takes place inside tunnels where the tunnel walls confine the flow around the products during impingement. Similarly, jet impingement cooling in a frost-free refrigerator occurs around confining walls and shelves. It is imperative, then, that research is directed toward jet impingement processes on bodies in confined space, representative of many such applications.

Very recently, Imraan and Sharma [11] reported on their initial studies on jet impingement heat transfer from a confined cylinder, where the influence of the distance between confining walls H, relative to the cylinder diameter d, for $z/w = 5$ and $d/w = 1$ was investigated. The research reported in this paper is an extension to the work described in [11] and seeks to present analysis and data on jet impingement heat transfer from a circular cylinder in a confined space for varying parameters of H/d, z/w, and d/w. Several confining wall separation-distance-H-to-cylinder-diameter ratios H/d, cylinder-diameter-to-slot-width ratios d/w, and a range of distance from jet-exit-to-cylinder-to-nozzle-width ratios z/w were investigated over the Reynolds number range of 1000–12,000 for a contoured orifice. Experimental data for heat transfer from a cylinder in uniform crossflow, and for a cylinder in a nonconfined space, were also obtained to serve as reference against which heat transfer for the slot-jet configurations in a confined space could be compared. CFD modeling was also conducted for a selected number of configurations for flow visualization purposes in order to aid explanation of experimental results.

II. Experimental Apparatus and Procedure

The apparatus for the study of slot-jet impingement heat transfer from a circular cylinder in a confined space included components for flow metering, jet generation, cylinder support, and confinement. A heated cylinder was also fabricated. These are now described in detail, together with some discussions on the experimental procedure, quantification of heat leakages, and uncertainties in data.

A. Flow and Jet Generation

As schematically shown in Fig. 1, the jet was generated by directing supply air flow, through a Meriam flowmeter, into the plenum containing a baffle plate and a screen and then through the contoured orifice with a thickness of 10 mm for impingement on the heated cylinder. A variable speed blower was used to develop the necessary air supply pressure and flow. The air volume flow rate was measured with the Meriam flowmeter. The total flow capacity of the system was limited to 0.052 m^3s^{-1}. The uncertainty in the measured flow rate was evaluated and found to be approximately 7% for the flow system. The plenum chamber was 450 mm high and 350 mm wide, with the same depth (normal to the figure) as the length of the heated cylinder of 160 mm. The contoured nozzle, having a contour radius of 8 mm, was constructed of Perspex and polished to provide smooth surfaces. The baffle plate in the plenum served to decelerate the flow from the plenum supply inlet, and it was designed together with the screen to provide near-unidirectional flow to the nozzle and help attain a symmetrical flow through the orifice. Maximum velocities in the plenum were calculated to be approximately 0.93 ms^{-1}.

B. Heated Cylinder

The heated cylinder was constructed from a 19-mm-diam aluminum rod with a length of 160 mm. A 2-mm-diam hole was drilled through the center of the rod, over its entire length.

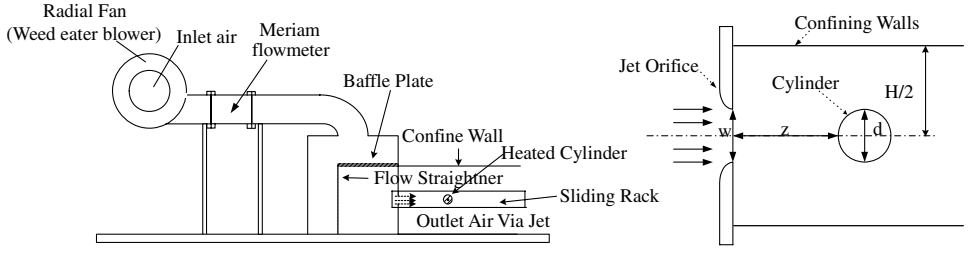

Fig. 1 Schematic illustration of the experimental setup.

Magnesium-oxide-coated constantan wire was drawn through the center hole, and the remaining space was filled with magnesium oxide. The constantan heating wire was connected to a larger-gauge electrical supply wire, as close to the cylinder as possible. The electrical supply wires were connected to a precision direct-current power supply, which provided the electrical power for ohmic heating. The total power dissipation was then calculated as the product of the measured current flow and voltage drop, which was approximately 11 W for the entire experiment. Four thermocouples were embedded underneath the surface of the cylinder, midway between the two ends. Four very fine grooves at 90° separations were milled along the axis of the aluminum cylinder to allow the thermocouple wires to be located within. These allowed temperature variations around the circumference of the cylinder to be measured from the four T-type thermocouples that were embedded. The grooves were filled with aluminum-based epoxy coating and then polished to make a smooth surface. Polishing reduces emissivity and thus minimizes radiation heat transfer. The thermocouple wires were terminated and connected to a high-resolution temperature data acquisition system capable of resolving temperatures to within 0.4°C. A thermocouple was also placed inside the plenum, upstream of the nozzle exit, for measuring the jet exit temperature T_∞. The maximum Biot number for the cylinder, based on measured average heat-transfer coefficients, was found to be 0.01, indicating that the cylinder was isothermal. The isothermal nature of the cylinder surface was further confirmed by temperature measurements during the tests. The maximum temperature variation in all experiments was less than 5.8% of the difference between the average cylinder and the jet temperatures $(\bar{T}_\theta - T_\infty)$.

C. Benchmarking

To provide benchmark heat-transfer data for the case of the cylinder in uniform crossflow, the heated cylinder was modified for use in a low-speed (0–17 ms^{-1}) low-turbulence (less than 2%) wind tunnel. The wind-tunnel measurements permitted confirmation of the experimental setup and procedure against the widely accepted cylinder-in-crossflow correlation of Churchill and Bernstein [12]:

$$\overline{Nu} = 0.3 + \frac{0.62Re^{1/2}Pr^{1/3}}{[1 + (0.4/Pr)^{2/3}]^{1/4}}\left[1 + \left(\frac{Re}{282,000}\right)^{5/8}\right]^{4/5} \quad (1)$$

Further tests were then conducted for jet impingement heat transfer from a cylinder without confinement. This permitted comparisons with the accepted jet impingement heat transfer from a cylinder correlation of McDaniel and Webb [6],

$$\overline{Nu} = BRe^m \quad (2)$$

where B and m are given in Table 1 for various slot-to-cylinder-spacing z/w and cylinder-diameter-to-slot-width ratios d/w. These were then used as the basis for evaluating the enhancement or decline of heat transfer from the slot-jet impingement configuration in various confinements over the full range of Reynolds numbers studied here.

Table 1 Constants for empirical correlation of Eq. (2), from [6]: contoured orifice

	$d/w = 2.0$			$d/w = 1.0$			$d/w = 0.66$	
z/w	B	m	z/w	B	m	z/w	B	m
1	0.65	0.48	0.5	0.49	0.54	0.33	0.62	0.51
3	0.44	0.54	1.5	0.49	0.54	1.0	0.6	0.51
5	0.33	0.58	2.5	0.45	0.55	1.66	0.53	0.53
7	0.30	0.59	3.5	0.41	0.56	2.33	0.57	0.52
9	0.28	0.59	4.5	0.41	0.56	3.0	0.54	0.53
11	0.28	0.59	5.5	0.37	0.58	3.66	0.53	0.54

D. Evaluation of Convection Heat-Transfer Coefficients

The average heat-transfer coefficient was calculated from the measured power dissipated ($\dot{Q}_{\mathrm{diss}}$ = voltage drop × current), calculated radiation loss $\dot{Q}_{\mathrm{rad}}$, and measured conductive losses $\dot{Q}_{\mathrm{cond}}$ through the ends and wires, the cylinder surface area A_S, and the measured temperatures as

$$\bar{h} = \frac{\dot{Q}_{\mathrm{conv}}}{A_S(\bar{T}_\theta - T_\infty)} = \frac{(\dot{Q}_{\mathrm{diss}} - \dot{Q}_{\mathrm{rad}} - \dot{Q}_{\mathrm{cond}})}{A_S(\bar{T}_\theta - T_\infty)} \quad (3)$$

where $\bar{T}_\theta$ is the average of the four temperatures measured on the surface of the heated cylinder. The average Nusselt number was then determined as

$$\overline{Nu} = \frac{\bar{h}d}{k} \quad (4)$$

As in the correlations of Churchill and Bernstein [12] and McDaniel and Webb [6], the thermophysical properties of air were evaluated at the film temperature, $(\bar{T}_\theta + T_\infty)/2$.

To quantify end-conduction losses $\dot{Q}_{\mathrm{cond}}$, temperature drops were measured along specified lengths of supply and voltage measurement wires at each end of the cylinder during uniform crossflow tests in the wind tunnel. Conduction losses were calculated at each Reynolds number, using the conduction rate equation. Radiation losses $\dot{Q}_{\mathrm{rad}}$ were estimated, using temperature measurements; however, these were found to be insignificant when compared with the conduction losses. From a range of such measurements, it was established that the losses were between 12 and 15% of the supply power, depending on the Reynolds number. Appropriate corrections were therefore applied to obtain the convective heat transfer from the cylinder surface, which were then used in the analysis.

E. Experimental Investigations

In the present study, there are four geometric parameters that describe the experimental configuration. These are the cylinder diameter d, the nozzle or the jet width w, the nozzle-to-cylinder spacing z, and the distance between the two confining walls H. Heat-transfer studies were conducted for a range of slot-width-to-cylinder-diameter ratios d/w (cylinder diameter $d = 19$ mm), a range of slot-to-cylinder-distance-to-slot-width ratios z/w of 1–9, and a range of Reynolds numbers and confinements H/d. The Reynolds number in this study is based on the average jet exit velocity V (determined from the orifice cross-sectional area and the metered total air flow rate) and the cylinder diameter, $Re = Vd/\nu$. Note that the Reynolds number is based on cylinder diameter rather than slot width 1) to provide consistency with previous data (e.g., McDaniel and Webb [6]), and 2) to allow comparison with the limiting case of heat transfer from a cylinder in uniform crossflow at the same velocity. The comparison between slot jet and uniform crossflow heat transfer is then made on the basis of slot-jet exit velocity being identical to the freestream velocity for uniform crossflow.

F. Complimentary Computational Fluid Dynamics Simulations for Flow Visualization

CFD modeling was applied in order to gain some insight into the flow behavior in different confinement situations and to aid in the understanding of the results obtained from experimentation. CFD served as a complimentary tool to aid flow visualization. As long as Nusselt number trends were in line with experimental data, we had confidence in its use in this manner. Transient state simulations in two dimensions of the heat transfer from a slot air jet impinging on a cylinder in a confined domain were made using the commercial CFD software package CFX 5.7.1 (ANSYS Workbench 9.0). This software is based on the finite-volume code, and further details may be found in [13]. The computational domain consisted of a region of flow to the contoured nozzle and the confined space in which the cylinder was located. The confining and other walls were modeled as adiabatic walls with a no-slip condition. To make the model robust, the exiting plane was assigned as an opening, at zero pressure relative

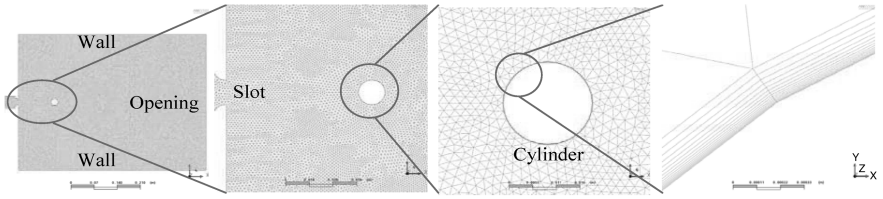

Fig. 2 CFD computational domain for $H/d = 22$ with some mesh details.

to the atmosphere (see Fig. 2). The cylinder had a diameter of 20 mm, and a range of slot-jet widths were examined. For the cylinder surface, the default wall function within ANSYS CFX [13] was applied, with an inflation layer setting through which 20 layers were specified within the expected thickness of the boundary layer. The CFD modeling was also informed by the content of [9,10,14]. The impinging jet was assumed to be 5% turbulent when exiting the slot, this being consistent with turbulence levels of 3–7%, measured with a COBRA four-hole pressure probe during experiments. As discussed elsewhere [9], the shear stress transport turbulence model [14] with automatic wall treatment was used in the simulation. As in experiments, the Reynolds number was based on the average jet velocity and the diameter of the cylinder. The mesh consisted of tetrahedral control volumes with appropriate settings for inflation layers near the cylinder and the walls, in order to resolve the conditions in the boundary-layer regions. The number of elements was maintained at approximately 650,000 for all the simulations, and the element size ranged between 1–2 mm. The temperature of the inflow was 25°C, and the surface temperature of the cylinder was set to 50°C. All except one simulation involved only heat transfer from the surface of the cylinder in this manner, and not within the cylinder. A simulation was run to additionally model the heat transfer within the aluminum cylinder, and it was verified that the cylinder surface was indeed nearly isothermal, as found in experiments. For the slot-jet impingement in a nonconfined space, the wall boundary conditions were replaced with openings.

III. Results and Discussions

A. Validation of Experimental Methodology

Figures 3 and 4 compare the Nusselt numbers obtained from experimental tests with those from the accepted correlations in Eqs. (1) and (2), respectively, for a cylinder in uniform crossflow and for a slot jet impinging on a cylinder in a nonconfined space. In these plots, data for cylinder-diameter-to-slot-width ratios d/w of 1.0 and 2.0 are included. Figure 3 shows that the experimental data for uniform crossflow are in excellent agreement with the accepted Nusselt number correlation of Churchill and Bernstein [12]. The maximum and average error between the experiment and the correlation of Churchill and Bernstein [12] was 3.7 and 0.8%, respectively. For slot-jet impingement heat transfer, data for both d/w ratios in Figs. 3 and 4 show that there is also good agreement with the correlation of McDaniel and Webb [6], with some deviation observed at higher Reynolds numbers. This is believed to be arising from differences in the nozzle profiles. McDaniel and Webb [6] have shown from their experimentation that Nusselt numbers for jet impingement are indeed sensitive to the nozzle profile. Nevertheless, the maximum and minimum differences between the experiment and

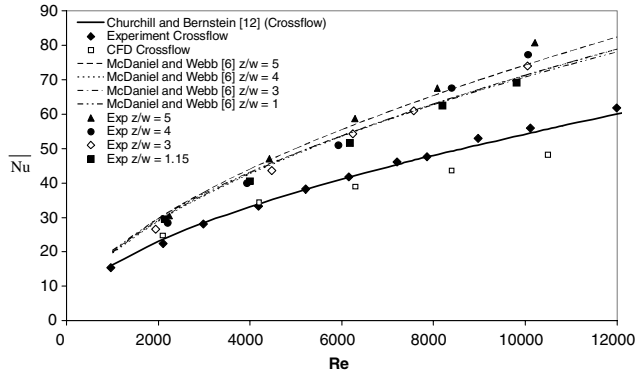

Fig. 3 Nusselt numbers for cylinder in uniform crossflow and in jet impingement without confinement, for $d/w = 1$.

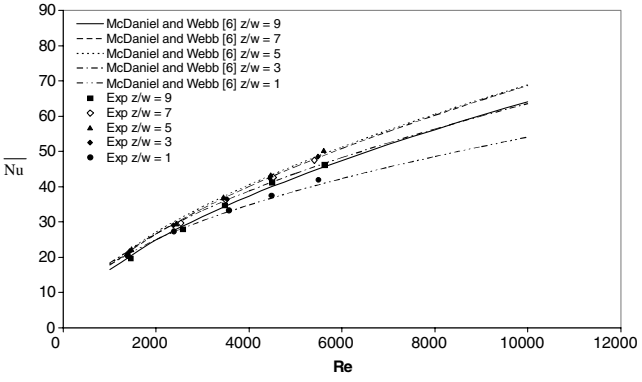

Fig. 4 Nusselt numbers for cylinder in uniform crossflow and in jet impingement without confinement, for $d/w = 2$.

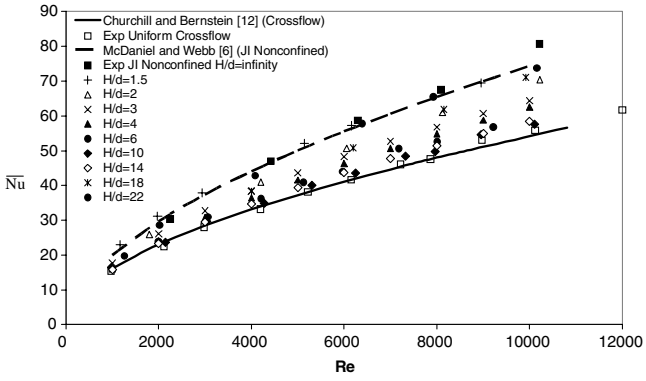

Fig. 5 Experimental Nusselt number against Reynolds number for slot-jet impingement on a circular cylinder in varying confinement H/d, fixed $d/w = 1.0$ and $z/w = 5$.

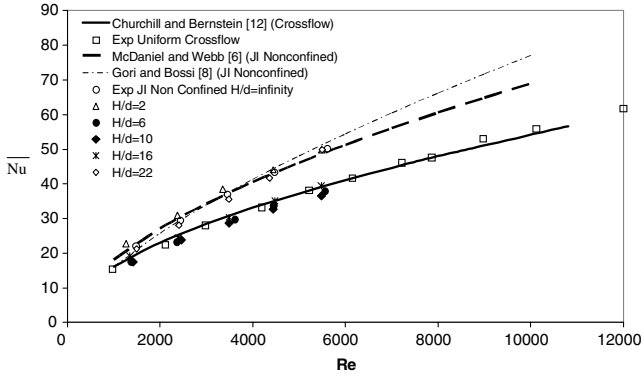

Fig. 6 Experimental Nusselt number against Reynolds number for slot-jet impingement on a circular cylinder in varying confinement H/d, fixed $d/w = 2.0$ and $z/w = 5$.

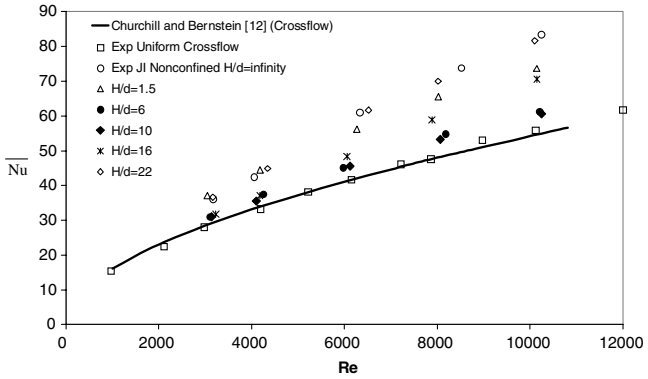

Fig. 7 Experimental Nusselt number against Reynolds number for slot-jet impingement on a circular cylinder in varying confinement H/d, fixed $d/w = 0.66$ and $z/w = 6$.

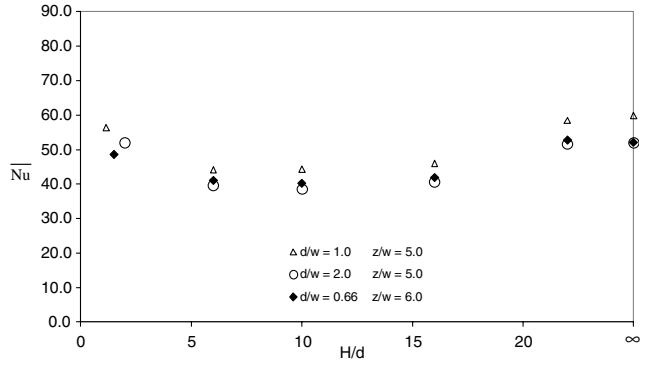

Fig. 8 Experimental Nusselt numbers against confinement H/d for jet impingement on a cylinder at a fixed Reynolds number of 6000, different d/w and z/w.

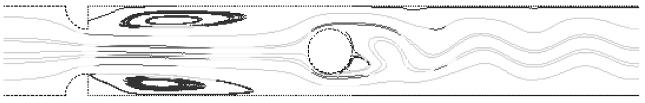

Fig. 9 Streamlines for $H/d = 2$ ($d/w = 1$ and $z/w = 5$).

Eq. (2) are only 5.6 and 0.2%, respectively. These provide obvious validation to the experimental methodology used here and confidence in the tests that followed. It is important to note that the maximum possible uncertainties in the Nusselt number and the Reynolds number were estimated to be 15 and 10%, respectively.

Figure 3 also includes the CFD-calculated Nusselt numbers for uniform crossflow. While the trends from CFD are in agreement with experimental data, the actual Nusselt numbers are underestimated: in particular, at Reynolds numbers above 8000. There are, possibly, a number of reasons for this: one being the two-dimensional CFD modeling not being able to capture the full three-dimensional characteristics of the jet, and any cylinder vortex shedding at high Reynolds numbers. However, since the trends are correct and the discrepancies are minimal at a Reynolds number of 6000, the CFD model was deemed acceptable for visualization studies to help explain the experimental data. Hence, all CFD visualizations reported in this paper are for a Reynolds number of 6000.

B. Influence of Confinement H/d

Figure 5 compares average Nusselt numbers obtained from the experiment for various confinements H/d and fixed $d/w = 1$ and $z/w = 5$. Similarly, Fig. 6 presents results for $d/w = 2$ and $z/w = 5$, while Fig. 7 presents results for $d/w = 0.66$ and $z/w = 6$. In these plots, measured data for uniform crossflow and jet impingement without confinement are also included. It should be noted that, in Fig. 7, which is for $d/w = 0.66$ and $z/w = 6$, there are no published data available for a circular cylinder in a nonconfined space.

The most significant observations from Figs. 5 and 6 are that the measured Nusselt numbers, for the most part, at various confinements H/d lie between those for uniform crossflow and slot-jet impingement in a nonconfined space. This might be a surprising result, as it would have been expected that confining walls rendered the jet and flow around the cylinder to be constrained and perhaps increase heat transfer, not reduce it. Exceptions to this are observed at the smallest $H/d = 1.5$ for $d/w = 1.0$ and $H/d = 2.0$ for $d/w = 2.0$, where the Nusselt numbers at Reynolds numbers below 4000 are somewhat higher than for the corresponding nonconfined cylinder, but they are within the 15% maximum error levels estimated for the Nusselt numbers in the experiments.

To understand the trends better, the measured Nusselt numbers are presented in Fig. 8, against confinement H/d, for different d/w at a Reynolds number of 6000. This shows some clear trends as follows:

1) The Nusselt number Nu is highest at the smallest confinement H/d of 1.5 (i.e., with the most blockage to flow).

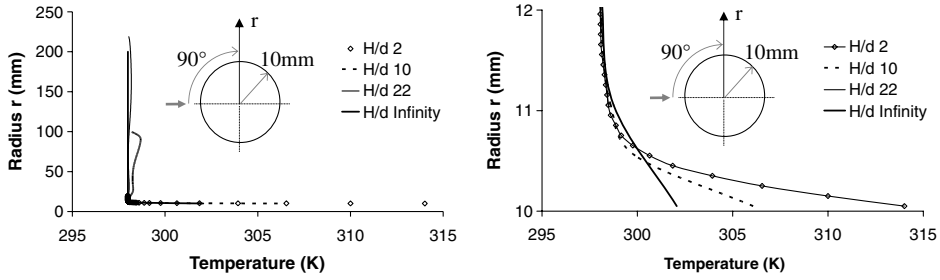

Fig. 10 Temperature profiles at 90° ($d/w = 1$ and $z/w = 5$).

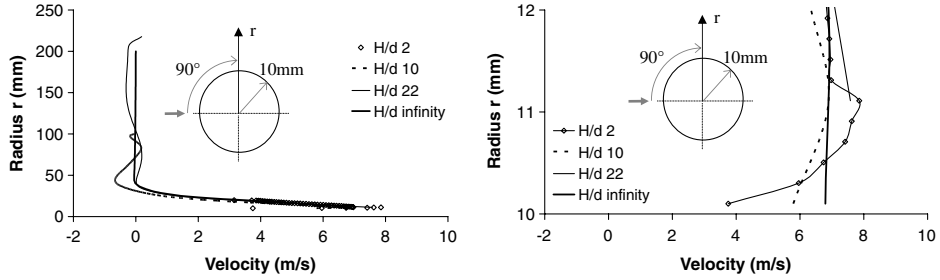

Fig. 11 Velocity profiles at 90° ($d/w = 1$ and $z/w = 5$).

Table 2 Entrainment analysis from CFD

	Mass flow rate $\times 10^3$ kg s^{-1}			
H/d	Plane	Inlet	Entrainment, %	Temp., °C
2	0.651	0.651	0	25.00
10	0.833	0.651	28	25.15
22	0.848	0.651	30	25.04
Infinity	0.861	0.651	32	25.00

2) The Nu reduces as H/d increases from 1.5 to 6.

3) The Nu remains nearly constant between H/d values of 6 to 14; however, the lowest Nu was recorded for a $H/d = 10$.

4) Between an H/d of 14 and 22, Nu increases. Interestingly, this trend, as well as the minimum-in-average Nusselt number at $H/d = 10$, was consistent across different d/w ratios.

To explain these interesting observations, flow visualization was carried out, using the results from CFD modeling for various configurations. The transient CFD simulation results used and presented here are all for a Reynolds number of 6000. The streamlines of flow in Fig. 9 at $H/d = 2$ ($d/w = 1.0$ and $z/w = 5$) show evidence of vortex shedding, which is known to induce vigorous mixing in the wake region of the cylinder. A close examination of the boundary-layer region of the cylinder at a 90° azimuth, shown in Figs. 10 and 11, reveals the highest temperature gradient, as well as velocities in the near-surface region for this case, as compared with other confinement H/d cases, which is not unexpected. Clearly, then, these flow characteristics lead to enhanced convection heat transfer from the surface, hence the Nusselt numbers for the smallest H/d values were found to be the highest.

For $H/d = 10$, at which Nusselt numbers and, hence, heat transfer were found to be a minimum, the streamlines at a number of time steps in Fig. 12 reveal a very complex unsteady flow behavior. There is evidence of the alternate formation and shedding of large flow structures on either side of the cylinder, in tandem with bistable switching of the jet between the two confining walls. The switching of the jet to one side generates a large region of recirculation (i.e., a large vortex between the cylinder and the opposite confining wall appears, which is subsequently shed) as the jet flaps across the cylinder toward the other confining wall. When the jet is switched to the other wall, a large vortex is formed between the cylinder and the first wall, which is subsequently shed as the jet flaps back, and the cycle repeats.

Jet switching or flapping across the cylinder means that the jet is never impinging fully on the cylinder, contrary to the situation found for other confinements. Furthermore, the effect of the large flow structures (i.e., large vortices) is to circulate some of the warm air back to the cylinder). The temperature profiles in Fig. 10 reveal that the air temperature along a radial line, at 90° azimuth, between radii of 20 and 100 mm, is highest for this case. To understand the degree of influence of the recirculating air (or entraining air for $H/d=$ infinity; that is, for no confinement), CFD postprocessing was used to establish the amount of recirculation (or entrainment) and the corresponding average air temperature going through a plane $0.5d$ upstream of the cylinder. The plane was of extent $3d$ high across the domain. Table 2 shows the results of this analysis for various H/d configurations. It is evident that approximately 30% of the mass flow rate toward the cylinder is due to the recirculation for H/d of 10 and 22, or due to the entrainment for $H/d =$ infinity. Furthermore, for $H/d = 10$, Table 2 shows that the average air temperature through the reference plane is slightly higher than the rest. As a consequence of these, and of jet switching, the heat-transfer rate and, therefore, the Nusselt number for the case $H/d = 10$, is found to be the smallest when compared with those for $H/d = 1.5$ or 2.

In Figs. 13a and 13b, the streamlines of flow and temperature contours for H/d of 22 show periodic vortex shedding from the cylinder and recirculation or entrainment of air, much the same as that for a jet impinging on a cylinder in a nonconfined space. Consequently, the Nusselt numbers for this case are very similar to that for a nonconfined cylinder.

C. Influence of Jet-Exit-to-Cylinder Spacing z/w with Confinement H/d

Figures 14–16 show a Nusselt number variation with z/w for $d/w = 0.66$, 1.0, and 2.0, and a Reynolds number of 6000, at a number of confinements H/d. A number of significant observations can be made from these results. First, for the nonconfined cylinder, a maximum in the Nusselt number is observed to occur at a z/w of five, which is in agreement with McDaniel and Webb [6], who found that a

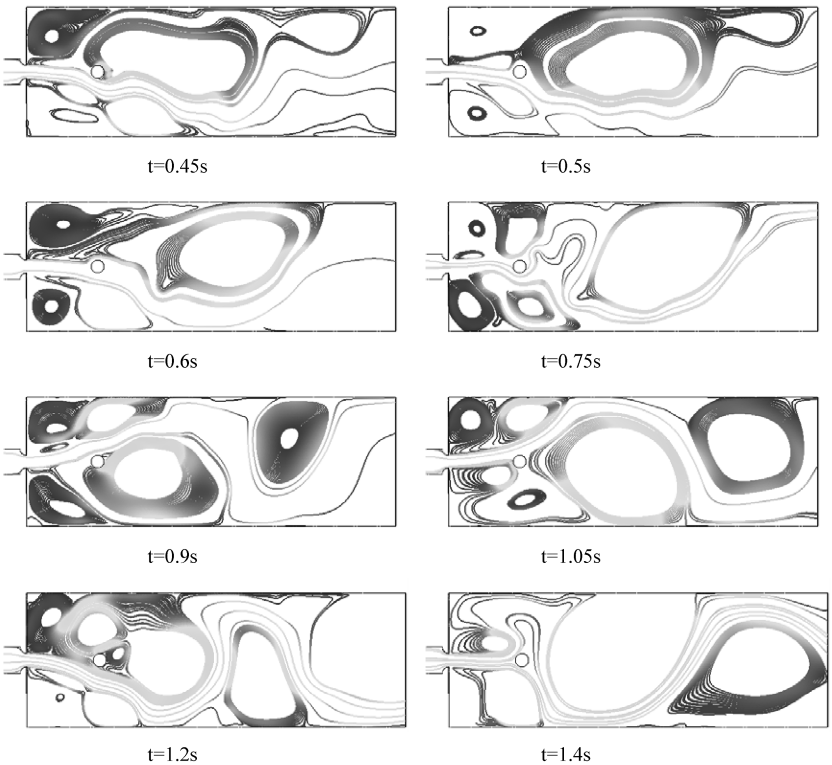

Fig. 12 Streamlines at various time steps for $H/d = 10$ ($d/w = 1$ and $z/w = 5$).

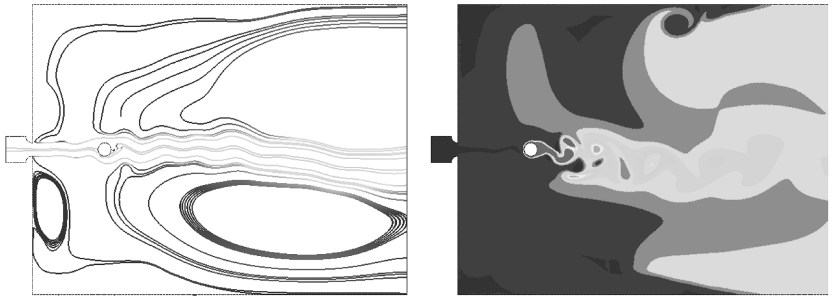

a) b)

Fig. 13 CFD flow visualization for $H/d = 22$ ($d/w = 1$ and $z/w = 5$): a) streamlines, and b) temperature contour map.

maximum occurs at $2 \leq z/w \leq 6$. This was attributed to the spacing $z/w = 5$, corresponding to the cylinder being located at the tip of the potential core of the jet, as illustrated in Fig. 17, where the air velocities were not diminished while having high turbulence levels due to the shear layer between the potential core and the quiescent air. At smaller spacing $z/w < 5$, the cylinder encounters a larger portion of the nonturbulent potential core and, at the same time, a smaller portion of the turbulent shear layer, leading to reduced heat transfer. On the other hand, at larger spacing $z/w > 5$, the cylinder is located beyond the potential core, where the air velocities are much reduced, leading to a reduction in heat transfer.

When the flow around the cylinder is confined, a maximum in the Nusselt number is similarly observed to occur at a z/w of five for all cases except the H/d of 1.5 (and one case of H/d of 22). This is again attributed to the location of the cylinder, relative to the potential core of the jet. At the smallest spacing $z/w = 1$ and most confinement $H/d = 1.5$, a large value of the Nusselt number was measured, which exceeds that found for the case of nonconfined cylinder. This is believed to be due, not only to a significant area of impingement, as the potential core is wide at $z/w = 1$, but also to the small passageway around the cylinder, causing the flow to be accelerated, as compared with that for larger values of H/d. These, together with the intense mixing brought about by vortex shedding, evident already in Fig. 9, are believed to cause significant enhancement in heat transfer. Furthermore, the Nusselt number variation with H/d, observed earlier for a z/w of five (see Figs. 6–8) is also found for all values of z/w studied here.

Some further observations can be made from Figs. 14–16. Whilst Fig. 14 for $d/w = 1$ shows that Nusselt numbers for the nonconfined cylinder and the confined case $H/d = 22$ are very similar, Figs. 15 and 16 for $d/w = 0.66$ and 2.0, however, do not show this trend. This is believed to be due to the onset of jet instability. On a number of occasions during experimentation, it was observed that the jet becomes unstable and continuously flaps across the cylinder between the confining walls. This phenomenon was mostly observed in confinements $H/d > 10$ and spacings $z/w > 5$. It is clearly evident from this observation that jet flapping was mostly taking place for higher H/d cases: for example, for $H/d = 22$ at $d/w = 0.66$ and 2.0. It is obvious that, when this happens, the jet does not effectively impinge on the cylinder, hence the heat transfer, and therefore the Nusselt number will be lowered. It was also observed that, for an H/d of 22 at $d/w = 1.0$, jet flapping was not present; therefore, the Nusselt number (see Fig. 14) is only slightly lower than that for a nonconfined cylinder. However, for $d/w = 0.66$ at an H/d of 22, there is a significant drop in Nusselt number, as shown in Fig. 15. Figure 16 for $H/d = 22$ at $d/w = 2.0$ shows that, for $z/w > 5$, there is again a significant drop in the Nusselt number when compared with the nonconfined cylinder, which could be attributed to the jet condition.

D. Influence of Cylinder-Diameter-to-Slot-Width Ratio d/w with Confinement H/d

Figure 18 shows that the Nusselt number is the highest for $d/w = 1.0$ for several confinements H/d at a relative spacing $z/w = 5$ and $Re = 6000$. For confinements of H/d of two, 22, and infinity

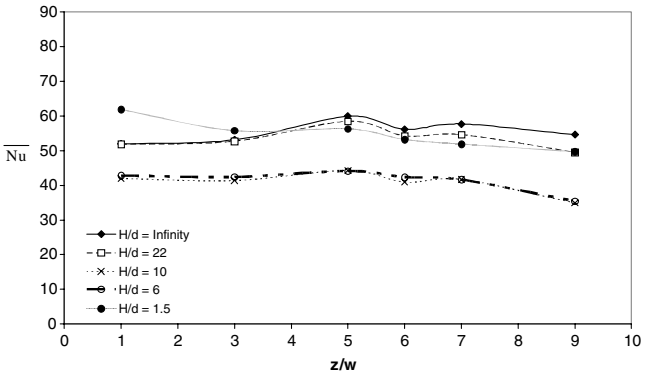

Fig. 14 Nusselt numbers with z/w, at a range of H/d, for $d/w = 1$ and $Re = 6000$.

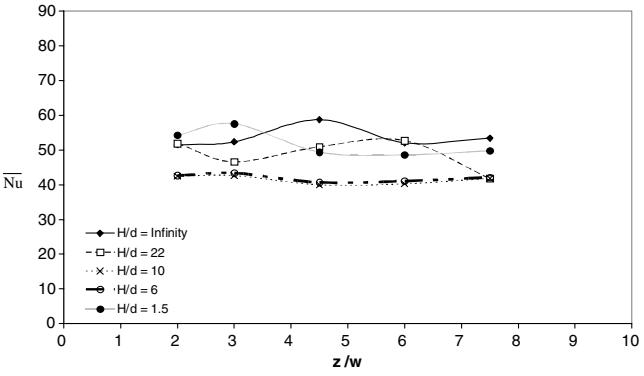

Fig. 15 Nusselt numbers with z/w, at a range of H/d, for $d/w = 0.66$ and $Re = 6000$.

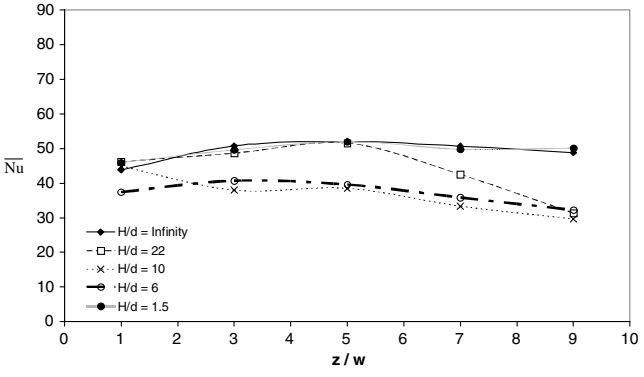

Fig. 16 Nusselt numbers with z/w, at a range of H/d, for $d/w = 2$ and $Re = 6000$.

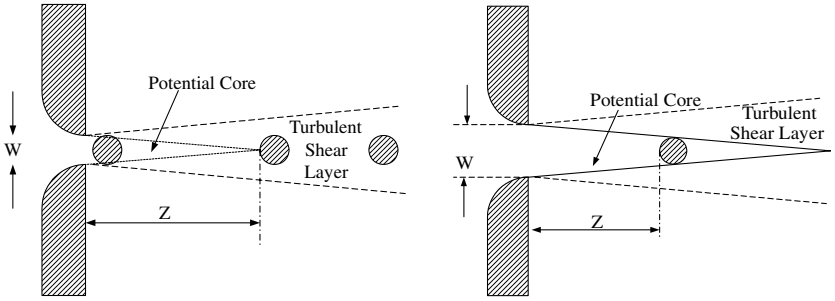

a) $d/w = 1.0$ **b) $d/w = 0.66$**

Fig. 17 Cylinder location relative to the potential core of the jet [6].

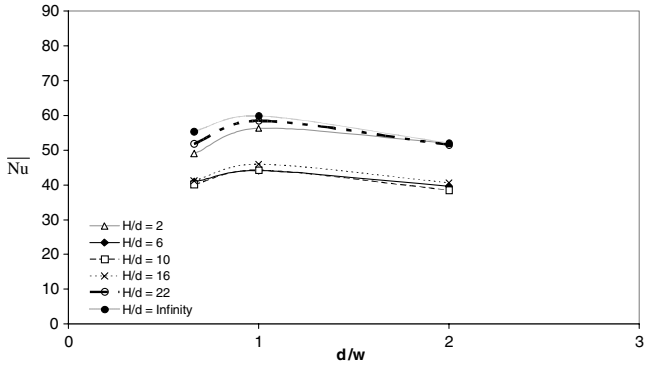

Fig. 18 Nusselt number versus d/w at $z/w = 5$, $Re = 6000$, and a range of H/d.

(nonconfined space), the Nusselt number is higher than those with an H/d of 6, 10, and 16. Furthermore, the Nusselt numbers are very close to each other for an H/d of 6, 10, and 16 at all values of d/w. For $d/w = 2$ at H/d of two, 22, and infinity (nonconfined space), the Nusselt numbers are very similar. These trends are consistent with earlier observations. Furthermore, CFD analysis was used to confirm that jet flapping also occurs at d/w of 0.66 and two for confinements H/d in the vicinity of 10.

We note that the data shown in Fig. 18 are those for $z/w = 5$. As discussed earlier, it was found that the maximum heat transfer occurs at $z/w = 5$ for most of the cases experimented in this research. For the case of $d/w = 1.0$ (i.e., $z = 5d$ and $z/w = 5$), the cylinder jet flow structure will be similar to that shown in Fig. 17a. However, when the slot width w is increased, so that $d/w = 0.66$ (with z still fixed at $5d$ but now $z/w = 10/3 < 5$), Fig. 17b best describes the flow behavior. This means that the cylinder with $d/w = 1.0$ is located at the tip of the potential core (Fig. 17a) and is cooled effectively by the unaffected approach flow and the high turbulence in the shear layer at the boundaries of the potential core. On the other hand, the cylinder with $d/w = 0.66$ lies entirely in the low-turbulence potential core region (Fig. 17b), is unaffected by turbulence in the shear layer, and, hence, has a somewhat lower heat-transfer rate and Nusselt number.

IV. Conclusions

Characteristics of heat transfer due to a slot jet of air from a contoured nozzle (of width w), impinging on a circular cylinder (diameter d), located between confining walls (at varying separation distance H apart), and at a range of spacing z from the jet exit were studied experimentally and computationally for Reynolds number Re in the range of 1000–12,000. Reference measurements were also made with the same cylinder in uniform crossflow in a wind tunnel. The results reveal that, while the slot jet impinging on a cylinder in confined space generally yields higher average heat-transfer rates, relative to the uniform crossflow case; these are, however, almost always found to yield lower heat-transfer rates in comparison with corresponding slot-jet impingement without confining walls. A few exceptions to these trends were, however, found at low Reynolds numbers. It is therefore concluded that jet impingement does not always enhance heat-transfer rate, but it may, in fact, reduce it under conditions in which the impingement target is located in the midst of confining walls.

On a number of occasions, it was found that, for confinements H/d between 10 and 16 and jet-exit-to-cylinder distance $z/w > 5$, the jet becomes unstable and starts to periodically flap across the cylinder, switching between the confining walls, in tandem with vortex shedding from the cylinder. This interesting flow behavior corresponds with the low values of heat transfer that were measured, since jet flapping reduces the effectiveness of impingement. Nevertheless, for the cases studied, it was found that, for the range of confinement spacings studied, the Nusselt number is maximized for z/w in the range of four to five. Furthermore, with respect to the cylinder-diameter-to-jet-width ratio, it is found that for all cases of confinement, the Nusselt number is maximum for $d/w = 1$. These findings are consistent with the trends for a nonconfined cylinder.

In summary, the influence of confining walls around the cylinder has a significantly detrimental impact on the flow and, therefore, the heat-transfer rates with jet impingement. The reduction in heat-transfer rates with confining walls implies that a jet impingement heat-transfer system, designed using data obtained for jet impingement on a nonconfined cylinder, could compromise the effectiveness of the system and may have a large bearing on the quality, efficiency, and productivity, as well as on the health and safety aspects, of products and processes.

Acknowledgment

This research was funded by the Guaranteed Financial Support Scheme, School of Engineering, the University of Auckland, New Zealand.

References

[1] Jambunathan, K., Lai, E., Moss, M. A., and Button, B. L., "A Review of Heat Transfer Data for Single Circular Jet Impingement," *International Journal of Heat and Fluid Flow*, Vol. 13, No. 2, 1992, pp. 106–115. doi:10.1016/0142-727X(92)90017-4

[2] Narayanan, V., Seyed-Yagoobi, J., and Page, R. H., "An Experimental Study of Fluid Mechanics and Heat Transfer in an Impinging Slot Jet Flow," *International Journal of Heat and Mass Transfer*, Vol. 47, Nos. 8–9, 2004, pp. 1827–1845. doi:10.1016/j.ijheatmasstransfer.2003.10.029

[3] Sparrow, E. M., and Alhomoud, A., "Impingement Heat Transfer at a Circular Cylinder Due to an Offset or Non-Offset Slot Jet," *International Journal of Heat and Mass Transfer*, Vol. 27, No. 12, 1984, pp. 2297–2305. doi:10.1016/0017-9310(84)90088-7

[4] Kang, S. H., and Greif, R., "Flow and Heat Transfer to a Circular Cylinder with a Hot Impinging Air Jet," *International Journal of Heat and Mass Transfer*, Vol. 35, No. 9, 1992, pp. 2173–2183. doi:10.1016/0017-9310(92)90061-V

[5] Bartoli, C., Di Marco, P., and Faggiani, S., "Impingement Heat Transfer at a Circular Cylinder Due to a Submerged Slot Jet of Water," *Experimental Thermal and Fluid Science*, Vol. 7, No. 4, 1993, pp. 279–286. doi:10.1016/0894-1777(93)90051-J

[6] McDaniel, C. S., and Webb, B. W., "Slot Jet Impinging Heat Transfer from Circular Cylinders, *International Journal of Heat and Mass Transfer*, Vol. 43, No. 11, 2000, pp. 1975–1985. doi:10.1016/S0017-9310(99)00267-7

[7] Gori, F., and Bossi, L., "On the Cooling Effect Of an Air Jet Along the Surface of a Cylinder," *International Communications in Heat and Mass Transfer*, Vol. 27, No. 5, 2000, pp. 667–676. doi:10.1016/S0735-1933(00)00148-2

[8] Gori, F., and Bossi, L., "Optimal Slot Height in the Jet Cooling of a Circular Cylinder," *Applied Thermal Engineering*, Vol. 23, No. 7, 2003, pp. 859–870. doi:10.1016/S1359-4311(03)00025-5

[9] Olsson, E. E. M., Ahrné, L. M., and Trägårdh, A. C., "Heat Transfer from a Slot Air Jet Impinging on a Circular Cylinder," *Journal of Food Engineering*, Vol. 63, No. 4, 2004, pp. 393–401. doi:10.1016/j.jfoodeng.2003.08.009

[10] Olsson, E. E. M., Ahrné, L. M., and Trägårdh, A. C., "Flow and Heat Transfer from Multiple Slot Air Jets Impinging on Circular Cylinders," *Journal of Food Engineering*, Vol. 67, No. 3, 2005, pp. 273–280. doi:10.1016/j.jfoodeng.2004.04.030

[11] Imraan, M., and Sharma, R. N., "Jet Impingement Heat Transfer in a Frost-Free Refrigerator: The Influence of Confinement," *International Journal of Refrigeration*, Vol. 32, No. 3, 2009, pp. 515–523. doi:10.1016/j.ijrefrig.2008.06.009

[12] Churchill, S. W., and Bernstein, M. A., "A Correlating Equation for Forced Convection from Gases and Liquids to a Cylinder in Crossflow," *Journal of Heat Transfer*, Vol. 99, Series C, No. 2, May 1977, pp. 300–306.

[13] ANSYS CFX Ver. 5.7.1 Reference Material, ANSYS, Inc., Canonsburg, PA, Nov. 2004.

[14] Menter, F. R., "Two-Equation Eddy-Viscosity Turbulence Models for Engineering Applications," *AIAA Journal*, Vol. 32, No. 8, 1994, pp. 1598–1604. doi:10.2514/3.12149